Synchronizability of double-layer dumbbell networks

Cite as: Chaos **31**, 073101 (2021); doi: 10.1063/5.0049281
Submitted: 3 March 2021 · Accepted: 17 June 2021 ·
Published Online: 2 July 2021

Juyi Li,[1,2] Yangyang Luan,[3] Xiaoqun Wu,[1,2,4,a)] and Jun-an Lu[1,2]

AFFILIATIONS

[1]School of Mathematics and Statistics, Wuhan University, Hubei 430072, China
[2]Research Center of Complex Network, Wuhan University, Hubei 430072, China
[3]School of Mathematical Science, Anhui University, Hefei 230601, China
[4]Hubei Key Laboratory of Computational Science, Wuhan University, Hubei 430072, China

[a)]**Author to whom correspondence should be addressed:** xqwu@whu.edu.cn

ABSTRACT

Synchronization of multiplex networks has been a topical issue in network science. Dumbbell networks are very typical structures in complex networks which are distinguished from both regular star networks and general community structures, whereas the synchronous dynamics of a double-layer dumbbell network relies on the interlink patterns between layers. In this paper, two kinds of double-layer dumbbell networks are defined according to different interlayer coupling patterns: one with the single-link coupling pattern between layers and the other with the two-link coupling pattern between layers. Furthermore, the largest and smallest nonzero eigenvalues of the Laplacian matrix are calculated analytically and numerically for the single-link coupling pattern and also obtained numerically for the two-link coupling pattern so as to characterize the synchronizability of double-layer dumbbell networks. It is shown that interlayer coupling patterns have a significant impact on the synchronizability of multiplex systems. Finally, a numerical example is provided to verify the effectiveness of theoretical analysis. Our findings can facilitate company managers to select optimal interlayer coupling patterns and to assign proper parameters in terms of improving the efficiency and reducing losses of the whole team.

Synchronization phenomena are of broad interest across disciplines and can be observed in natural, social, and technological systems. Over the past few decades, there have been numerous works on the synchronization of complex networks, but only a few of them have focused on the impact of multiplex networks on synchronizability. In this paper, we define a special double-layer dumbbell network in the context of company management and study its synchronizability under different interlayer coupling patterns using both analytical and numerical methods. The results are of practical significance, as company chairmen can utilize them to improve their management.

I. INTRODUCTION

Multiplex networks are of great theoretical and practical significance in the field of complex networks.[1–3] With the deepening study and increasing applications of complex networks, it has been gradually realized that most networks do not exist alone but are interconnected and interdependent with other networks. Recently, research on multiplex networks has been gaining more attention, including robustness,[4–6] information dissemination,[7–9] disease transmission,[10–18] synchronization,[19–29] control,[30–32] etc. Numerous achievements have shown that there are significant differences between multiplex networks and traditional networks. Although multiplex networks are of great importance and applicability, the relational study is still in its infancy.

Synchronization is one of the amazing collective behaviors found in nature. There have been several outstanding works on the synchronization of complex networks over the past few decades and large quantities of problems on the synchronization of single-layer networks have been explored,[33–36] but there are still many uncovered synchronization problems for multiplex networks worth studying.[37–45]

In this paper, a special two-layer network, called the double-layer dumbbell network, is proposed in the context of company or government management. This network can be a good demonstration of the information transmission between different departments

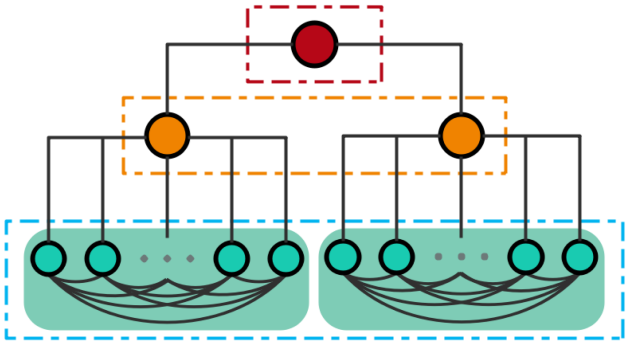

FIG. 1. Schematic diagram of a one-layer dumbbell network. Here, the red nodes represent company chairmen, the orange nodes represent department directors, and the green nodes represent department employees. In addition, the nodes in green shading are connected to each other and all connected to the director of their respective department; thus, a fully connected graph is formed within the department.

of a company or a government, i.e., the synchronization problem.[46,47] For a better understanding of the structure of our proposed double-layer dumbbell network, the schematic diagram of one layer is first displayed in Fig. 1. In our considered double-layer dumbbell network, each layer consists of $2N+3$ nodes, with one central node (i.e., company chairmen, the red nodes) connecting with another two nodes (i.e., department directors, the orange nodes), and the two nodes are fully connected with the other N peripheral nodes (i.e., department employees, the green nodes), respectively. These N peripheral nodes are also fully connected, and the nodes that represent company chairmen have no direct connection with the nodes that represent department employees. What is more, the two dumbbell layers connect by specific patterns, and this process of one-to-one interlayer connection can be regarded as information transmission online and offline in a company, or between two companies intercommunicated by chairmen, directors, and employees.

To explore the synchronizability of this system, the analytical expressions of the corresponding Laplacian matrix are derived theoretically for the double-layer dumbbell system with different interlink patterns, and then the impact of the interlink coupling strength on synchronizability of this double-layer dumbbell system is further studied. It is discovered that the connection between company chairmen for single-link coupling patterns and two interlinks from different departments for two-link coupling patterns exhibits the best synchronizability, both for unbounded and bounded synchronized regions. Finally, the dumbbell systems consisting of networks with other topologies and a numerical example with Rössler system being node dynamics are also considered. The accuracy and effectiveness of our theoretical analysis are all verified.

The layout of this paper is as follows. Section II presents the dynamic equation and the supra-Laplacian matrices. Section III explores the single-link coupling pattern and the two-link coupling pattern of double-layer dumbbell networks as well as specific analytical polynomials containing the largest and the smallest nonzero eigenvalues for single-link coupling patterns of general dumbbell network. Section IV illustrates the analytical and numerical results to characterize the synchronizability of double-layer dumbbell networks. Section V confirms the effectiveness of theoretical results by numerical examples. Finally, Sec. VI draws some conclusions and briefly discusses some possible future work.

II. PRELIMINARIES

We consider a multiplex network with M layers, each layer containing N nodes. The dynamic system of the ith node in the Kth layer can be described as[48]

$$\dot{x}_i^K = f\left(x_i^K\right) + a_K \sum_{j=1}^{N} w_{ij}^K H\left(x_j^K\right) + \sum_{L=1}^{M} d_i^{KL} \Gamma\left(x_i^L\right), \tag{1}$$

where $i = 1, 2, \ldots, N$, $K = 1, 2, \ldots, M$, $x_i^K \in \mathscr{R}^N$ is the state of the ith node in the Kth layer, $f(\cdot) : \mathscr{R}^N \to \mathscr{R}^N$ is a well-defined vector function representing the dynamic equation of nodes in the system, a_K is the intralayer coupling strength of the Kth layer. According to the definition, $W^K = (w_{ij}^K) \in \mathscr{R}^{N\times N}$ is the adjacency matrix of the Kth layer. Here, $w_{ij}^K = 1$ if node i is connected with node j ($j \neq i$) within the Kth layer, and $w_{ij}^K = 0$ otherwise. In addition, $w_{ii}^K = -\sum_{j=1, j\neq i}^{N} w_{ij}^K$; thus, $L^K = -a_K W^K$ is a Laplacian matrix. The continuous functions $H : \mathscr{R}^N \to \mathscr{R}^N$ and $\Gamma : \mathscr{R}^N \to \mathscr{R}^N$ represent intralayer and interlayer coupling functions, respectively, and d_i^{KL} is the interlayer coupling strength between the Kth layer and the Lth layer of the ith node. Similarly, $d_i^{KL} = 1$ if node i in the Kth layer is connected with node j ($j \neq i$) in the Lth layer, and $d_i^{KL} = 0$ otherwise. Let $d_i^{KK} = -\sum_{L=1, L\neq K}^{M} d_i^{KL}$; thus, it is clear that $D = (d_i^{KL}) \in \mathscr{R}^{M\times M}$ is a negative Laplacian matrix.

Let $\mathscr{L}$ be the supra-Laplacian matrix of the above system, $\mathscr{L}_{\text{Inter}}$ be the supra-Laplacian matrix indicating the interlayer topology, and $\mathscr{L}_{\text{Intra}}$ be the supra-Laplacian matrix representing the intralayer topology. Then, $\mathscr{L}$ can be denoted as

$$\mathscr{L} = \mathscr{L}_{\text{Inter}} + \mathscr{L}_{\text{Intra}}. \tag{2}$$

With D referring to the Laplacian matrix of the interlayer networks, the interlayer supra-Laplacian matrix can be written as

$$\mathscr{L}_{\text{Inter}} = D \otimes E_N, \tag{3}$$

where $\otimes$ is the Kronecker product and E_N is the $N \times N$ identity matrix.

The intralayer supra-Laplacian matrix of a multiplex network is defined as

$$\mathscr{L}_{\text{Intra}} = \begin{pmatrix} L^1 & 0 & \cdots & 0 \\ 0 & L^2 & \cdots & 0 \\ \vdots & \vdots & \ddots & \vdots \\ 0 & 0 & \cdots & L^M \end{pmatrix} = \bigoplus_{K=1}^{M} L^K, \tag{4}$$

where $K = 1, 2, \ldots, M$ and L^K is the Laplacian matrix of the Kth layer.

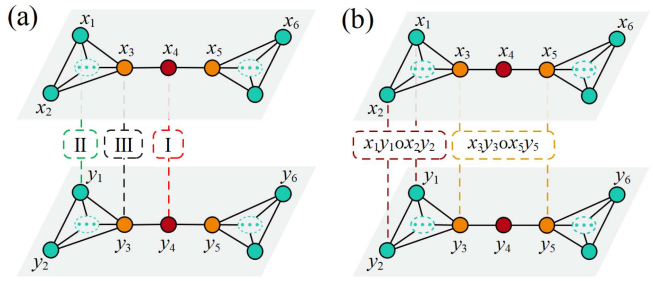

FIG. 2. Schematic diagram of single-link [panel (a)] and two-link [panel (b)] interlayer coupling patterns for a double-layer dumbbell network. The three single-link connection modes are denoted as I, II, and III in panel (a) for short. In addition, $x_1, x_2, x_3, x_4, x_5, x_6$ are selected as representative feature points taken in one layer of a double-layer dumbbell network, and their replicas in the other layer are denoted by $y_1, y_2, y_3, y_4, y_5, y_6$. In panel (b), the connection modes $x_1y_1 \circ x_2y_2$ and $x_3y_3 \circ x_5y_5$ can be regarded as the two interlayer patterns out of the seven two-link interlayer coupling patterns.

Taking our double-layer dumbbell network as an example, the node dynamics of this two-layer system can be written as Eq. (1) with $M = 2$. Then, for a double-layer dumbbell network with single-link coupling patterns shown in Fig. 2(a), the corresponding interlayer and intralayer supra-Laplacian matrix can be calculated as follows:

$$\mathscr{L}_{\text{Inter}} = \begin{bmatrix} dE_{cc} & -dE_{cc} \\ -dE_{cc} & dE_{cc} \end{bmatrix}, \quad \mathscr{L}_{\text{Intra}} = \begin{bmatrix} L^1 & 0 \\ 0 & L^2 \end{bmatrix}.$$

Furthermore, according to Eq. (2), one gets

$$\mathscr{L} = \begin{bmatrix} L^1 + dE_{cc} & -dE_{cc} \\ -dE_{cc} & L^2 + dE_{cc} \end{bmatrix},$$

where $d_i^{KL} = d$ here. In addition, E_{cc} represents a matrix in which the elements in the cth row and the cth column are 1, and the remaining elements are 0, where c denotes the number label of the currently connected node.

In the same way, for a double-layer dumbbell network with two-link coupling patterns shown in Fig. 2(b), the corresponding supra-Laplacian matrix can be obtained as follows:

$$\mathscr{L} = \begin{bmatrix} L^1 + d(E_{cc} + E_{kk}) & -d(E_{cc} + E_{kk}) \\ -d(E_{cc} + E_{kk}) & L^2 + d(E_{cc} + E_{kk}) \end{bmatrix},$$

where c and k denote the number labels of the currently connected nodes.

According to the method of the master stability function,[20] synchronizability of a network can be judged by observing the eigenvalues of its supra-Laplacian matrix. Above all, the eigenvalues of the supra-Laplacian matrix $\mathscr{L}$ for a connected multiplex network can be recorded as $0 = \lambda_1 < \lambda_2 \le \lambda_3 \le \cdots \le \lambda_{\max}$. Generally, we use λ_2 to evaluate the synchronizability of a network whose synchronized region is unbounded. The larger the λ_2 is, the better synchronizability the network has. In addition, for a network whose synchronized region is bounded, the ratio $R = \lambda_{\max}/\lambda_2$ determines the synchronizability. Contrary to the relationship of λ_2 to network synchronizability, the smaller the R is, the better synchronizability the network has.

In order to facilitate the following theoretical derivation, a special formula is given as follows:[49]

$$\begin{vmatrix} A & B \\ B & A \end{vmatrix} = |A + B||A - B|, \tag{5}$$

where A and B are $N \times N$ square matrices.

III. THEORETICAL ANALYSIS

For the double-layer dumbbell network, the nodes can be divided into three categories according to their actual attributes: company chairmen (represented by red nodes), department directors (represented by orange nodes), and department employees (represented by green nodes), respectively. In our work, two common interlayer coupling patterns are considered: one is single-link coupling and the other is two-link coupling. The influence of these two interlayer coupling patterns on the synchronizability of the double-layer dumbbell network is discussed as follows.

A. Single-link coupling pattern between layers

Due to the symmetry of the double-layer dumbbell network, there are three cases of single-link connection modes between layers, shown as I, II, and III in Fig. 2(a). Here, we first assume that the central node (i.e., company chairman) in each layer is connected to m departmental structures, and each department has N employees and one department director. Obviously, each layer of the dumbbell network has $m(N + 1) + 1$ nodes. Similarly, we can prove that there are still three cases of single-link connection modes between layers as mentioned above. Assuming that the intralayer coupling strength of each layer is a, and the interlayer coupling strength between layers is d, i.e., $a_1 = a_2 = a$ and $d_i^{KL} = d$ for these three interlayer connection modes about the general dumbbell model, the corresponding analytical expressions to characterize synchronizability are given as follows.

For connection mode I of the general dumbbell model, the smallest nonzero eigenvalue λ_2 and the largest eigenvalue $\lambda_{\max}$ are the minimum and maximum roots of the following equation, respectively, for all N, a, d and m:

$$\alpha^{2m(N-1)}\beta^{2(m-1)}\begin{Bmatrix}[(\lambda - ma)\beta - ma^2(\lambda - a)] \\ \times[(\lambda - ma - 2d)\beta - ma^2(\lambda - a)]\end{Bmatrix} = 0, \tag{6}$$

where $\alpha = \lambda - (N + 1)a$ and $\beta = \lambda^2 - (N + 2)a\lambda + a^2$ are substitution factors for short.

For connection modes II and III of the general dumbbell model, the analytical expressions containing λ_2 and $\lambda_{\max}$ of corresponding Laplacian matrices are listed, respectively, as follows:

$$\alpha^{(2m-1)(N-1)}\beta^{2m-3}\begin{Bmatrix}[(\lambda - ma)\beta - ma^2(\lambda - a)] \\ \times[\beta\psi - (m-1)a^2(\lambda - a)\varphi]\end{Bmatrix} = 0 \tag{7}$$

and

$$\alpha^{2m(N-1)}\beta^{2m-3}\begin{Bmatrix}[(\lambda - ma)\beta - ma^2(\lambda - a)] \\ \times\begin{bmatrix}[(\lambda - ma)\beta - (m-1)a^2(\lambda - a)] \\ \times[\beta - 2d(\lambda - a)] - 2a^2d^2(\lambda - a^2)\end{bmatrix}\end{Bmatrix} = 0, \tag{8}$$

where φ and ψ are substitution factors for short, and their mathematical expressions are as follows:

$$\varphi = \alpha^{N-1}(\alpha - a)\left[\lambda - 2d - \frac{2ad(N-1)}{\alpha} - \frac{a(2d-a)}{\alpha - a}\right],$$

$$\psi = (\lambda - ma)\varphi - a^2\alpha^{N-1}\left[\lambda - a - 2d - \frac{2ad(N-1)}{\alpha}\right].$$

For simplicity and clarity, we mainly focus on the double-layer dumbbell network with only two community structures, and the corresponding characteristic expressions can be obtained easily by means of setting $m = 2$ in Eqs. (6)–(8). Additionally, the double-layer dumbbell network described later is by default a structure with only two community structures in each layer.

Without loss of generality, one can assume that each dumbbell layer has $2N + 3$ nodes, the intralayer coupling strength is a, and the interlayer coupling strength is d, so the smallest nonzero eigenvalue λ_2 and the largest eigenvalue $\lambda_{\max}$ of the supra-Laplacian matrix for this double-layer network satisfy the following analytical expressions. For connection mode I, one has

$$\lambda^3 - (Na + 4a + 2d)\lambda^2 + (2Na + 2Nd + 3a + 4d)a\lambda - 2a^2d = 0. \tag{9}$$

For connection mode II, one has

$$\begin{aligned}\lambda^6 &- (3Na + 7a + 2d)\lambda^5 + (3N^2a + 16Na + 4Nd + 18a + 14d)a\lambda^4 \\ &+ (N^2a + 8Na + 2Nd + 13a + 10d)a\lambda^3 \\ &+ (2N^3a + 10N^2a + 6N^2d + 20Na + 32Nd + 13a + 42d)a^3\lambda^2 \\ &- (2N^2a + 4N^2d + 5Na + 18Nd + 3a + 20d)a^4\lambda \\ &+ 2a^5d(N+1) = 0.\end{aligned} \tag{10}$$

For connection mode III, one has

$$\begin{aligned}\lambda^5 &- 2(Na + 3a + d)\lambda^4 + (N^2a + 4Na + 2Nd + 17a + 10d)a\lambda^3 \\ &+ (2N^2a + 7Na - 6Nd + 3a - 8d)a^2\lambda^2 \\ &+ (3Na^2 + 4Nad + 8a^2 + 10ad - 2d^2)a^2\lambda \\ &+ a^4(2d^2 - 2d - a) = 0.\end{aligned} \tag{11}$$

By computing the roots of Eqs. (9) and (11), one can easily obtain the smallest nonzero and largest eigenvalues for the three single-link connection modes of the double-layer dumbbell network. Therefore, the synchronizability of the dumbbell network with different connection strategies can be evaluated by comparing their λ_2 and R.

B. Two-link coupling pattern between layers

Due to the symmetry of the double-layer dumbbell network, there are seven cases of two-link connection modes between layers. As shown in Fig. 2(b), when x_1 is connected with y_1 and x_2 is connected with y_2, we denote this connection mode as $x_1y_1 \circ x_2y_2$, and it is obviously one of the seven connection modes. Apart from this, another six connection modes can be listed as $x_1y_1 \circ x_3y_3$, $x_1y_1 \circ x_4y_4$, $x_1y_1 \circ x_5y_5$, $x_1y_1 \circ x_6y_6$, $x_3y_3 \circ x_4y_4$ and $x_3y_3 \circ x_5y_5$, respectively.

Similar to the calculation principle in Sec. III A, one can evaluate the synchronizability of the double-layer dumbbell network in two-link coupling patterns, as obtaining the analytical equations which contains the largest and the smallest nonzero eigenvalues of corresponding Laplacian matrices. However, it is difficult to derive an explicit expression of λ_2 or $\lambda_{\max}$ as a function of d because their corresponding characteristic equations are high-order polynomials. Through the error analysis in the later section, it can be found that the analytical solutions can be represented approximately by some simplified numerical solutions, in terms of reducing the calculation and time complexity. As a result, the synchronizability of the double-layer dumbbell network in two-link coupling patterns can be explored more efficiently.

IV. EXPERIMENTAL RESULTS

In this section, analytical and numerical results are provided for investigating the synchronizability of double-layer dumbbell networks. Since the main focus of our work is to explore the relationship between the synchronizability of the dumbbell network and the interlayer coupling strength, we set intralayer coupling strength $a = 1$ unless there are other statements. Moreover, considering the connection between the members of a company is closer when communicating online and there is no clear concept of superior–subordinate relation like offline communication; hence, a fully connected graph of the dumbbell network is also taken as the intralayer structure. Then, a double-layer network consisting of one dumbbell layer and one fully connected graph mentioned above can be constructed to study its synchronization. Finally, the relation between λ_2 and interlink weight d of single-link coupling patterns for double-layer dumbbell network is also investigated under the analytical and numerical method.

Primarily, consider a double-layer network formed by two dumbbell networks interconnected with the two previously described coupling patterns, i.e., single-link and two-link coupling patterns. The schematic illustration for three connection modes of single-link coupling is displayed in Fig. 2(a) denoted as I, II, and III.

Figure 3 displays λ_2 and R for the double-layer dumbbell system varying with respect to interlayer coupling strength d. Here, N is set to be 3, which means the size of each dumbbell layer is 9. Panels (a) and (b) are obtained analytically from Eqs. (9)–(11) for the three single-link connection modes.

From panel (a) of Fig. 3, we find that λ_2 increases rapidly with small d for any single-link connection mode, and the increase slows down when d reaches a certain value. This means that for the double-layer dumbbell network with connection mode I, its synchronizability can be quickly enhanced with increasing d at small values and finally almost levels off when d is large enough. It is also observed that $\lambda_2^{\mathrm{I}} > \lambda_2^{\mathrm{III}} > \lambda_2^{\mathrm{II}}$ for any $d > 0$, which means that connection mode I is the best option for maximizing synchronizability for single-link coupling, while connection mode II is the worst one. It is worth emphasizing that this result contradicts the viewpoint in Ref. 50 , in which the interlayer connection between nodes with larger degrees leads to better synchronizability in a double-layer star network. In fact, the degree centrality is not accurate enough in

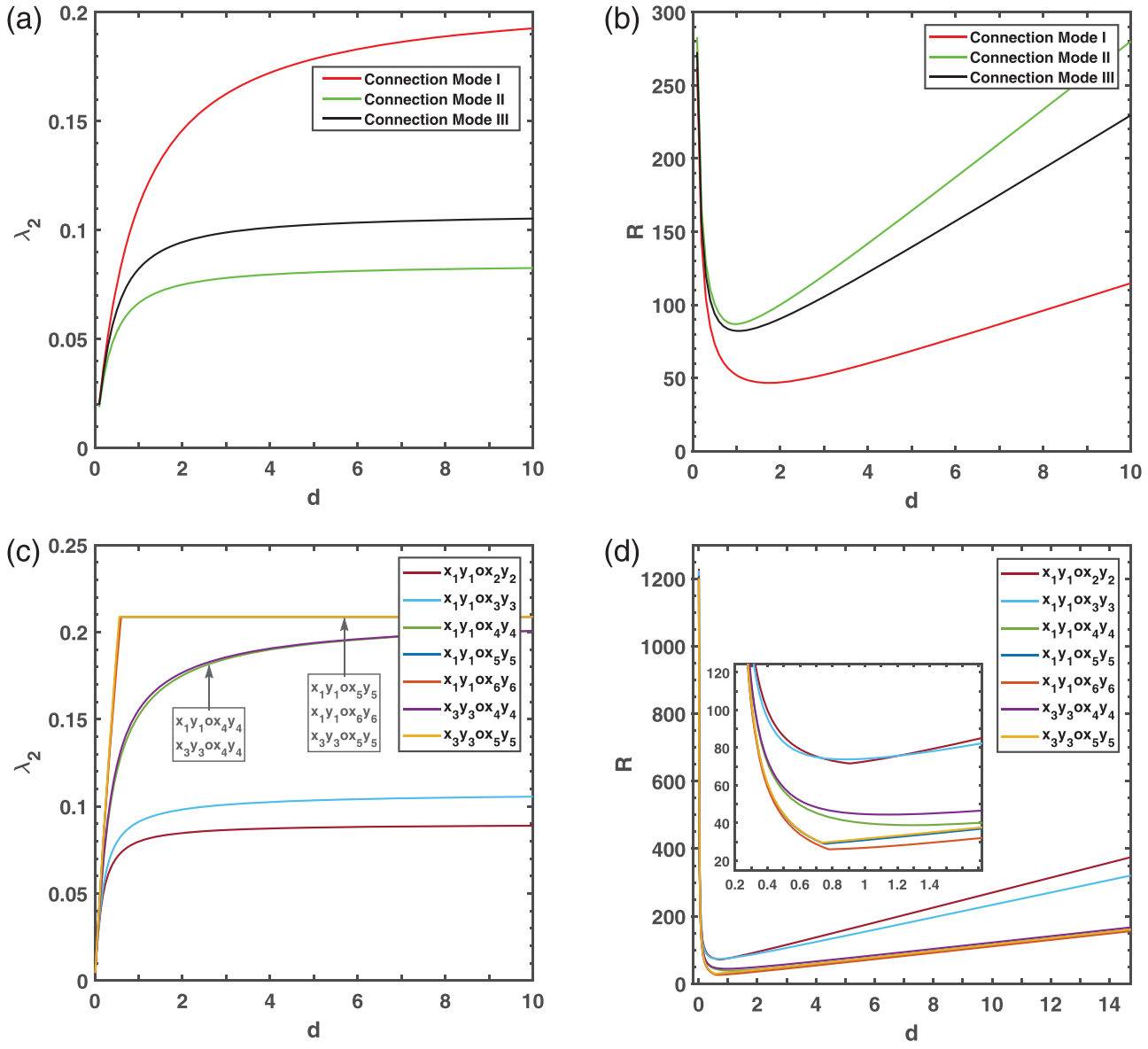

FIG. 3. Synchronizability of the dumbbell systems under the situation of single-link coupling and two-link coupling patterns of weight d. Here, $N = 3$. Panels (a) and (c) display λ_2 varying with d. Panels (b) and (d) display R varying with d. Panels (a) and (b) are obtained analytically from Eqs. (9)–(11), and (c) and (d) are obtained numerically from Laplacian matrices of the dumbbell network.

most cases while employing it to measure the influence of nodes, since only the number of nearest neighbors for one given node is considered. As shown in Table I, the centrality values of nodes are measured by the degree centrality,[51] the eigenvector centrality,[52,53] the closeness centrality,[54,55] and the betweenness centrality.[56,57] We find that the central node plays the most important role in closeness centrality and betweenness centrality, although it is the least important under the degree centrality and the eigenvector centrality. This result to some extent implies that the interaction between central nodes is more conducive to synchronization of the double-layer dumbbell network.

From panel (b) of Fig. 3, one can observe that for connection modes I, II, and III, R first decreases at a small d and then increases monotonically with d increasing. In addition, $R^{\mathrm{I}} > R^{\mathrm{III}} > R^{\mathrm{II}}$ exists for any $d > 0$. Therefore, if the synchronized region of a double-layer dumbbell network is bounded, its synchronizability

TABLE I. The centrality values of nodes in a single-layer dumbbell network, measured by the degree centrality (DC), the eigenvector centrality (EC), the closeness centrality (CC), and the betweenness centrality (BC). The best performance is highlighted in bold font for each identification algorithm.

Node[a]	DC	EC	CC	BC
1	2.6667	0.3275	0.4000	0.0000
2	2.6667	0.3275	0.4000	0.0000
3	2.6667	0.3275	0.4000	0.0000
4	**3.5556**	**0.3856**	0.5333	0.5357
5	1.7778	0.2427	**0.5714**	**0.5714**
6	**3.5556**	**0.3856**	0.5333	0.5357
7	2.6667	0.3275	0.4000	0.0000
8	2.6667	0.3275	0.4000	0.0000
9	2.6667	0.3275	0.4000	0.0000

[a]The nodes are labeled sequentially from left to right according to the arrangement shown in Fig. 1. For instance, the node labeled as 5 is the central node, the ones labeled as 4 and 6 are their adjacent nodes, i.e., department director, and the rest represent the department employees.

is enhanced first under connection modes I, II, and III, then reaches the maximum, and finally gets weakened. It is worth noting that connection mode I turns out to be the best synchronization option for single-link coupling patterns, no matter whether the synchronized region is unbounded or not.

Panels (c) and (d) of Fig. 3 are obtained numerically from Laplacian matrices of the double-layer dumbbell network, for seven two-link connection modes. It is observed from Fig. 3(c) that, $\lambda_2^{x_1y_1\circ x_5y_5} \approx \lambda_2^{x_1y_1\circ x_6y_6} \approx \lambda_2^{x_3y_3\circ x_5y_5} > \lambda_2^{x_1y_1\circ x_4y_4} \approx \lambda_2^{x_3y_3\circ x_4y_4} > \lambda_2^{x_1y_1\circ x_3y_3} > \lambda_2^{x_1y_1\circ x_2y_2}$ for any interlayer coupling strength d. Regardless of the two-link connection mode for the double-layer dumbbell network, the synchronizability increases fast and then reaches steady at a certain d. According to the connection modes that enable the double-layer dumbbell network to reach the strongest synchronizability, we can obtain that the selection of interlayer coupling between members from different departments benefits the promotion of network synchronizability. Additionally, the connection modes $\lambda_2^{x_1y_1\circ x_3y_3}$ and $\lambda_2^{x_1y_1\circ x_2y_2}$ lead to lower synchronizability, which may account for this coupling occurring in the same department.

From Fig. 3(d), it is clear that $R^{x_1y_1\circ x_2y_2} > R^{x_1y_1\circ x_3y_3} > R^{x_3y_3\circ x_4y_4} \approx R^{x_1y_1\circ x_4y_4} \approx R^{x_3y_3\circ x_5y_5} \approx R^{x_1y_1\circ x_6y_6} \approx R^{x_1y_1\circ x_5y_5}$ for any interlayer coupling strength d, which reflects the connection modes $x_1y_1 \circ x_2y_2$ and $x_1y_1 \circ x_3y_3$, have worse synchronizability than other modes if the synchronized region is bounded. These results, to some extent, may inspire engineers some constructive advice in terms of maximizing synchronizability and promoting the company's efficiency.

For the double-layer dumbbell network with a larger department size, the impact of interlayer coupling strength d on λ_2 and R is worth exploring. Suppose that the department size of each dumbbell layer is 50, which means the number of department employees N is equal to 49. The relevant results are shown in Fig. 4. Comparing Figs. 3 and 4, it is easy to find that the influence of different coupling patterns on network synchronizability has not changed. In others words, connection mode I for single-link coupling patterns and the links from different departments for two-link coupling patterns perform the best synchronizability, both in unbounded and bounded synchronized regions. Additionally, the network synchronizability in different interlink patterns of $N = 49$ is weaker than that of $N = 3$.

Given the above results, it is worthwhile to further investigate the relationship between network synchronizability and the size of the company department. Here, the network synchronizability varying with the size of the company department is displayed in Fig. 5, in terms of single-link coupling pattern. Figure 5(a) shows λ_2 varying with N while the interlink weight $d = 1$, and Fig. 5(b) shows the same while the interlink weight $d = 10$. It is observed that the synchronizability gets weakened with the department size increasing when the interlink coupling strength d is fixed. In addition, there is one point worth noting that the difference between the nodes with different categories (i.e., company chairman, department director, and department employee) gradually decreases with an increase in N. Moreover, it is also apparent that higher interlink strength gives greater superiority to connection mode I than connection modes II or III.

For dumbbell systems consisting of networks with other intralayer topologies, corresponding analytical expressions cannot be found easily. However, the synchronizability of such kind of dumbbell system can be carried numerically, as shown in Fig. 6, where the double-layer systems are composed of a dumbbell network and a corresponding fully connected network. Here, the size of department employees N is set to be 3 for a test. It is observed that connection mode I for single-link coupling patterns and connection mode $x_1y_1 \circ x_6y_6$ for two-link coupling patterns still perform better than other coupling cases. The results are similar to those for the double-layer dumbbell networks, suggesting that the previous analytical and numerical methods for the double-layer dumbbell network have a significant value of applicability.

Considering that the analytical solutions of Laplacian matrices are represented approximately by some simplified numerical solutions before; thus, it is essential to validate the rationality here. Figure 7 plots λ_2 varying with respect to d for three single-link connection modes. The black line, the red line, and the blue line in Fig. 7(a) represent the theoretical values of λ_2 obtained from the corresponding analytical expression, i.e., Eqs. (9)–(11), and the corresponding numerical result is shown in Fig. 7(b). The number of department employees N is 49 here. Obviously, the theoretical results are completely consistent with the numerical results. Therefore, the substitution is practical and effective for analyzing synchronizability of double-layer dumbbell networks, particularly when the analytical expression of λ_2 or $\lambda_{\max}$ is hard to derive.

This section can be concluded as follows. For a double-layer system composed of two dumbbell networks where each layer is connected according to different coupling patterns, the synchronizability is determined by the interlink weight d. For any connection mode, the synchronizability is enhanced continually with increasing d when the interlayer connection strength is weak. However, when the interconnection becomes strong enough (d exceeds some thresholds), the synchronizability increases much slower and is almost unaltered for the dumbbell network with increasing d. In addition, both the connection patterns and size of the network have a certain

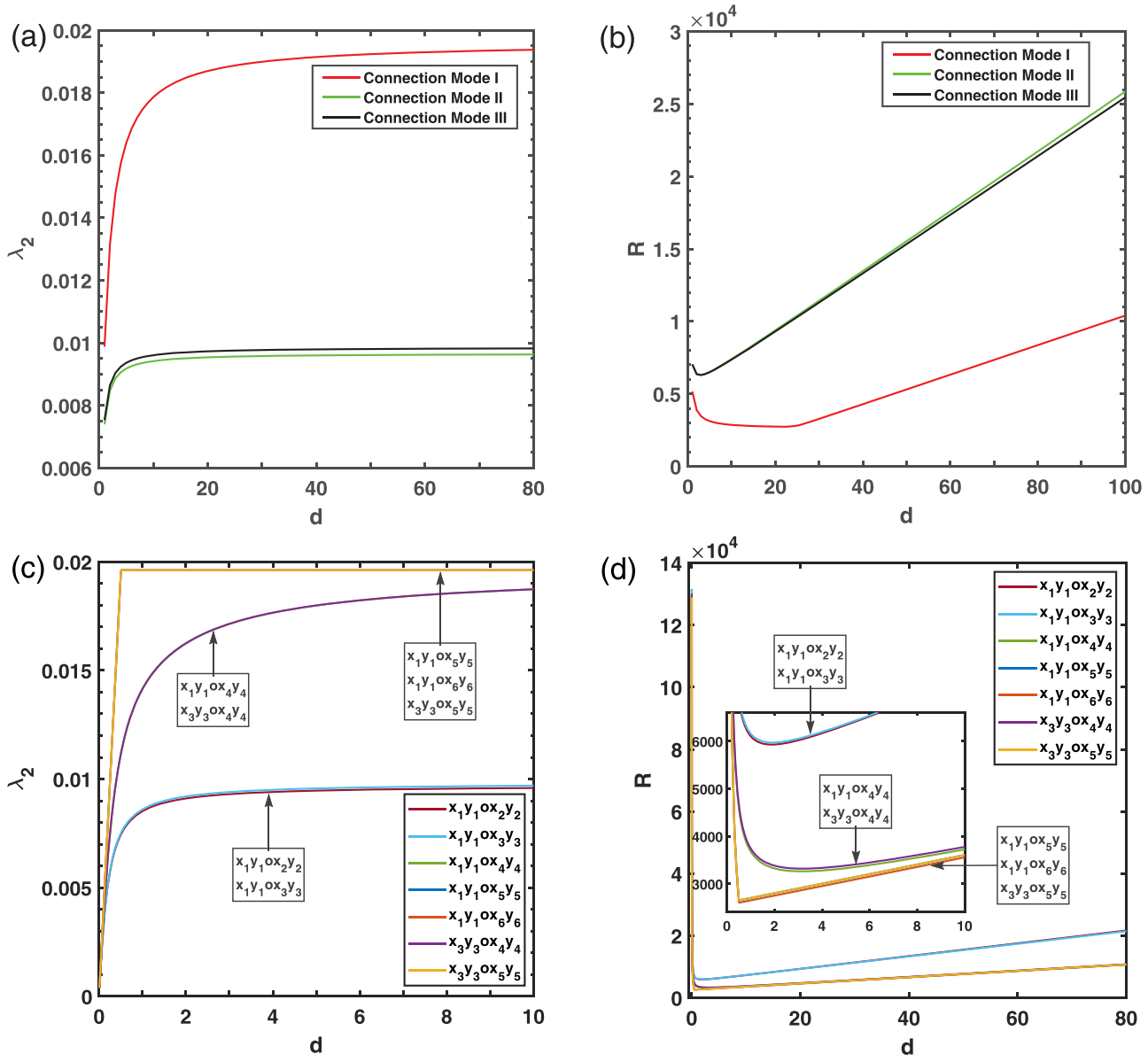

FIG. 4. Synchronizability of double-layer dumbbell system under the situation of single-link and two-link coupling patterns of interlink weight d. Here, $N = 49$. Panels (a) and (c) display λ_2 varying with d. Panels (b) and (d) display R varying with d. All these results are obtained numerically from Laplacian matrices of the double-layer dumbbell network.

impact on the synchronizability of this double-layer dumbbell system. Therefore, the results can provide engineers with an optimal design of interlink strength d for dumbbell networks composed of the systems with special background, in terms of maximizing synchronizability and minimizing control cost.

V. NUMERICAL SIMULATIONS

A numerical example is provided to illustrate the theoretical results. Consider a double-layer system formed by two dumbbell networks, each consisting of $2N + 3$ Rössler systems interconnected by two links, which is described by

$$\dot{x}_i(t) = f_i(t, x_i(t)) + \sum_{j=1}^{4N+6} d_{ij}\Gamma x_j(t), \quad i = 1, 2, \ldots, 4N + 6, \qquad (12)$$

where $f_{i1}(t, x_i(t)) = -x_{i2} - x_{i3}$, $f_{i2}(t, x_i(t)) = x_{i1} + 0.45x_{i2}$, $f_{i3}(t, x_i(t)) = 2 + x_{i3}(x_{i1} - 4)$, and $x_i(t) = (x_{i1}(t), x_{i2}(t), x_{i3}(t))^T$ is the state

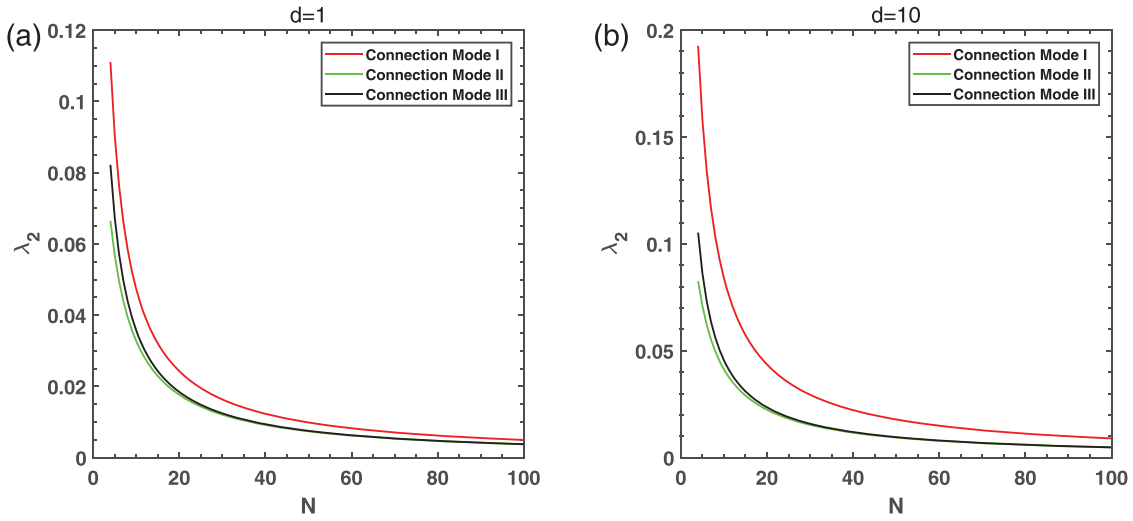

FIG. 5. Relation between λ_2 and the size of department employees N for double-layer dumbbell network. Here, we take the single-link coupling patterns as an example and discuss the two cases of interlink strength $d = 1$ [panel (a)] and $d = 10$ [panel (b)], respectively.

variable of the ith node; $f_i(t, x_i(t))$ is the dynamics equation of node i, Γ is the inner coupling matrix, and $A = (d_{ij})_{(4N+6)(4N+6)}$ is the coupling configuration matrix. If node i and node j are in the same layer and there is a link between them, then $d_{ij} = 1$; if nodes i and j are in different layers and there is a link connecting them, then $d_{ij} = d$; otherwise $d_{ij} = 0$. The diagonal elements of A are $d_{ii} = -\sum_{j=1,j\neq i}^{4N+6} d_{ij}, i = 1, 2, \ldots, 4N + 6$. To measure the coherence in this dumbbell system, the following complete synchronization error is introduced:

$$D(t) = \frac{1}{2}\sum_{i=1}^{4N+6}\sum_{j=1}^{3}\left(x_{ij} - \bar{x}_j\right)^2, \tag{13}$$

where $\bar{x}_j = [1/(4N + 6)]\sum_{i=1}^{4N+6} x_{ij}$ is the average state of the jth $(j = 1, 2, 3)$ variable of all nodes in the dumbbell system. In numerical simulations, the Runge–Kutta fourth-order method is

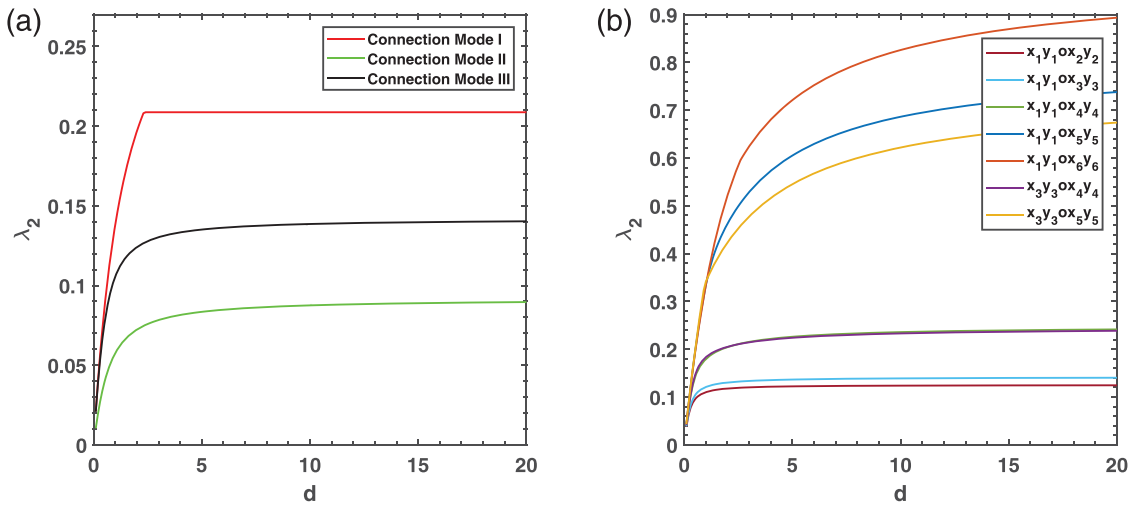

FIG. 6. Synchronizability of the duplex system consisting of a dumbbell network and a corresponding fully connected network interconnected by two links of weight d, for single-link coupling patterns [panel (a)] and two-link coupling patterns [panel (b)], respectively. Here, $N = 3$.

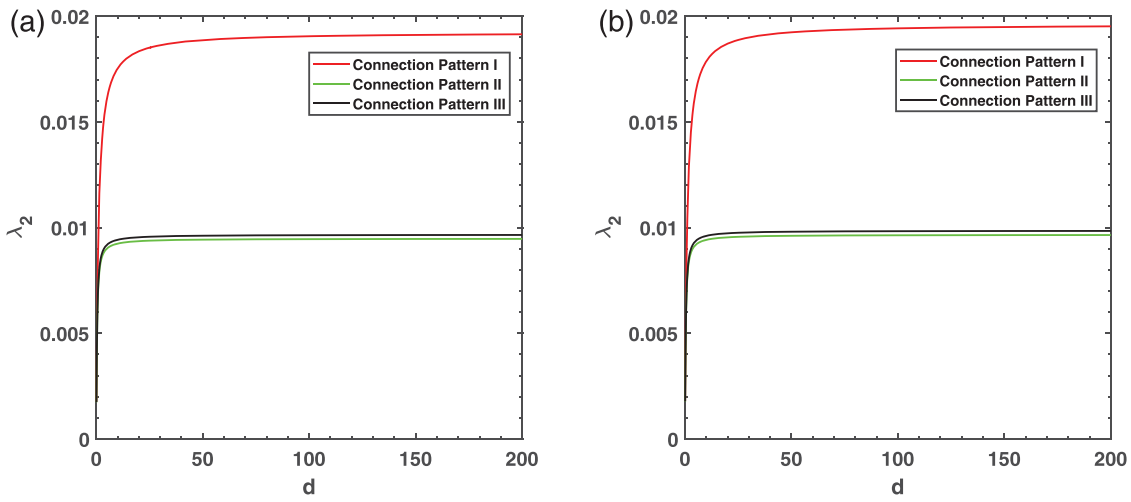

FIG. 7. Relation between λ_2 and interlink weight d of the single-link coupling patterns for the double-layer dumbbell network. For $N = 49$, panel (a): the theoretical values computed from the corresponding analytical expressions; panel (b): the numerical results calculated from Laplacian matrices of the double-layer dumbbell network.

employed to solve the ordinary differential equations, i.e., Eq. (12), with an equal time step of 0.1.

Figure 8 displays the synchronization errors varying with time for three single-link connection modes and seven two-link connection modes, where the layer size of double-layer dumbbell network is 9, the interlink weight $d = 5$, $\Gamma = \mathrm{diag}(1, 1, 1)$, and $D(t)$ is averaged over 20 realizations of randomly set initial values. It is seen from Fig. 8(a) that the system reaches complete synchronization in all single-link connection modes. Furthermore, from the inset, one can see that $D(t)$ of the connection mode I tends to zero first, while $D(t)$ of the connection mode II is the slowest to arrive at zero. It is again shown that connection mode I is the best way to facilitate synchronization from numerical perspectives, while connection mode II is the best way to inhibit it. Figure 8(b) shows that the dumbbell reaches complete synchronization in all two-link connection modes, and one can easily see from the inset that $D(t)$ of the connection modes $x_1y_1 \circ x_5y_5$, $x_1y_1 \circ x_6y_6$, $x_3y_3 \circ x_5y_5$ tends toward zero first, while $D(t)$ of the connection modes $x_1y_1 \circ x_2y_2$ and $x_1y_1 \circ x_3y_3$ is the slowest to arrive at zero. These results once again validate the view we got before.

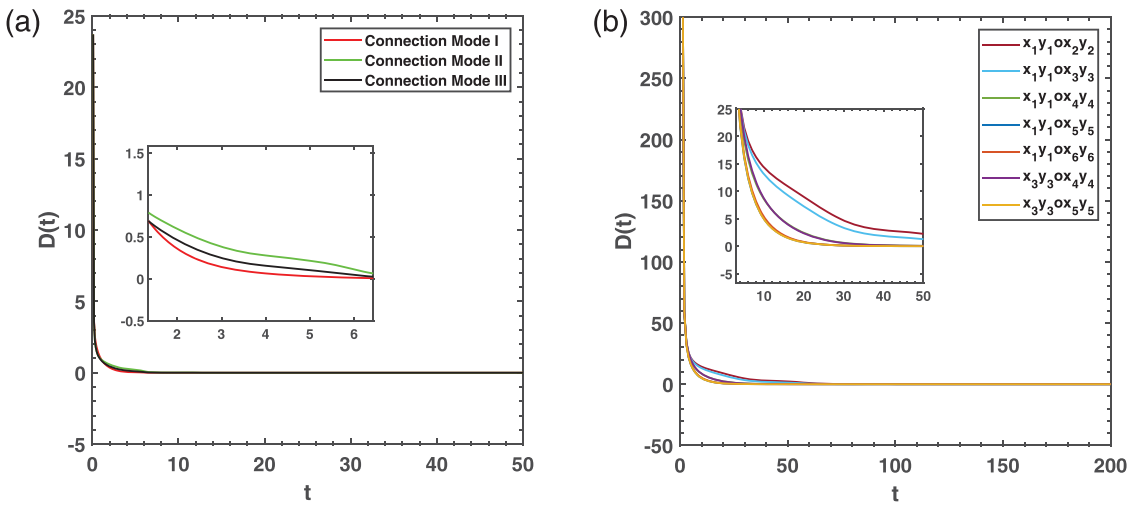

FIG. 8. Time evolution of synchronization errors of the dumbbell formed by two dumbbell networks, each layer consisting of 9 Rössler oscillators for single-link coupling patterns and 101 Rössler oscillators for two-link coupling patterns. Panel (a) is for three single-link connection modes with $d = 5$ and $a = 5$ and panel (b) is for seven two-link connection modes with $d = 5$ and $a = 5$. Here, $D(t)$ is averaged over 20 realizations of randomly set initial values.

VI. CONCLUSION AND DISCUSSION

It has been investigated that, for the double-layer system formed by two dumbbell networks interconnected with different coupling patterns, the role of nodes and coupling patterns between layers plays a crucial part in complete synchronization of the system. In addition, the weight of interlinks is also a key factor determining synchronizability. Analytical equations containing the largest and the smallest nonzero eigenvalues of the Laplacian matrix have been given for the double-layer dumbbell network with different interlayer coupling patterns. Analytical and numerical results show that increasing the interlink strength favors the synchronizability of the double-layer dumbbell network with unbounded synchronized regions, while for a network with bounded synchronized regions, there exists an optimum interlink strength that maximizes its synchronizability. In addition, the rules go beyond two dumbbell networks and are of general applicability to double-layer networks formed by other kinds of intralayer topologies. Finally, a numerical example of a network composed of Rössler systems is presented to illustrate our theoretical analysis. The findings can offer engineers the selection of optimal designs of interlayer coupling patterns and interlink strength for multiplex networks with either unbounded or bounded synchronized regions, such as in power grids, in terms of maximizing synchronizability and minimizing control cost.

So far, there remain many problems about multilayer networks to be solved. Based on our double-layer dumbbell network, a significant but challenging topic would be proposed about the synchronizability toward varying the number of interlayer connections or allocating directed couplings. In addition, only single-link and two-link interlayer coupling patterns are considered in our work, while dumbbell networks with more general interlayer coupling patterns are worthy of further exploration.[58] Therefore, more constructive situations and better feasible methods need to be examined. In addition, we usually study the relationship between the synchronizability of the dumbbell network and the interlayer coupling strength after fixing the network structure first so as to find a feasible way to maximize the synchronizability of the whole system. However, on the contrary, how can we maximize the synchronizability if we adjust the structure of one layer after fixing the interlink coupling pattern first?[59] Last but not least, whether the dumbbell structure can yield explosive synchronization under the right setup is also an interesting topic.[25] We hope our study can spark possible solutions to the above-mentioned problems or others in the near future.

ACKNOWLEDGMENTS

We would like to thank Miss Chen for polishing the manuscript. This work was supported in part by the National Key Research and Development Program of China under Grant No. 2018AAA0101100, the National Natural Science Foundation of China (NNSFC) under Grant No. 61973241, and the Natural Science Foundation of Hubei Province under Grant No. 2019CFA007.

DATA AVAILABILITY

The data that support the findings of this study are available from the corresponding author upon reasonable request.

REFERENCES

[1] J. Gómez-Gardeñes, I. Reinares, A. Arenas, and L. Mario Floría, "Evolution of cooperation in multiplex networks," Sci. Rep. **2**, 620 (2012).
[2] P. J. Mucha, T. Richardson, K. Macon, M. A. Porter, and J.-P. Onnela, "Community structure in time-dependent, multiscale, and multiplex networks," Science **328**, 876–878 (2010).
[3] F. Battiston, V. Nicosia, and V. Latora, "Structural measures for multiplex networks," Phys. Rev. E **89**, 032804 (2014).
[4] B. Min, S. Do Yi, K.-M. Lee, and K. I. Goh, "Network robustness of multiplex networks with interlayer degree correlations," Phys. Rev. E **89**, 42811 (2014).
[5] M. Kitsak, L. K. Gallos, S. Havlin, F. Liljeros, L. Muchnik, H. E. Stanley, and H. A. Makse, "Additional repulsion reduces the dynamical resilience in the damaged networks," Chaos **30**, 023132 (2020).
[6] Z. Chen, J. Wu, Y. Xia, and X. Zhang, "Robustness of interdependent power grids and communication networks: A complex network perspective," IEEE Trans. Circuits Syst. II **65**, 115–119 (2018).
[7] M. Kitsak, L. K. Gallos, S. Havlin, F. Liljeros, L. Muchnik, H. E. Stanley, and H. A. Makse, "Identification of influential spreaders in complex networks," Nat. Phys. **6**, 888–893 (2010).
[8] M. Nekovee, Y. Moreno, G. Bianconi, and M. Marsili, "Theory of rumour spreading in complex social networks," Physica A **374**, 457–470 (2008).
[9] Z. Zhang, C. Liu, X. Zhan, X. Lu, C. Zhang, and Y. Zhang, "Dynamics of information diffusion and its applications on complex networks," Phys. Rep. **651**, 1–34 (2016).
[10] M. E. J. Newman, "Spread of epidemic disease on networks," Phys. Rev. E **66**, 016128 (2002).
[11] Q. Wu and S. Chen, "Spreading of two interacting diseases in multiplex networks," Chaos **30**, 073115 (2020).
[12] C. Granell, S. Gomez, and A. Arenas, "Dynamical interplay between awareness and epidemic spreading in multiplex networks," Phys. Rev. Lett. **111**, 128701 (2013).
[13] C. Granell, S. Gómez, and A. Arenas, "Competing spreading processes on multiplex networks: Awareness and epidemics," Phys. Rev. E **90**, 012808 (2014).
[14] Y. Cheng, Z. Wang, C. Zheng, Q. Guo, Y. Shi, M. Dehmer, and Z. Chen, "A new coupled disease-awareness spreading model with mass media on multiplex networks," Inf. Sci. **471**, 185–200 (2019).
[15] W. Wang, Q. Liu, J. Liang, Y. Hu, and T. Zhou, "Coevolution spreading in complex networks," Phys. Rep. **820**, 1–51 (2019).
[16] D. Soriano-Panos, L. Lotero, A. Arenas, and J. Gomez-Gardenes, "Spreading processes in multiplex metapopulations containing different mobility networks," Phys. Rev. X **8**(3), 031039 (2018).
[17] J. T. Matamalas, S. Gomez, and A. Arenas, "Abrupt phase transition of epidemic spreading in simplicial complexes," Phys. Rev. Res. **2**, 012049(R) (2020).
[18] X. Wei, X. Wu, S. Chen, J. Lu, and G. Chen, "Cooperative epidemic spreading on a two-layered interconnected network," SIAM J. Appl. Dyn. Syst. **17**, 1503–1520 (2018).
[19] L. M. Pecora and T. L. Carroll, "Synchronization in chaotic system," Phys. Rev. Lett. **64**, 821 (1990).
[20] L. M. Pecora and T. L. Carroll, "Master stability functions for synchronized coupled systems," Phys. Rev. Lett. **80**(10), 2109–2112 (1998).
[21] Q. Wu and S. Chen, "Spreading of two interacting diseases in multiplex networks," Chaos **28**(1), 013110 (2020).
[22] A. Kumar, M. S. Baptista, A. Zaikin, and S. Jalan, "Mirror node correlations tuning synchronization in multiplex networks," Phys. Rev. E **96**, 062301 (2017).
[23] J. Sawicki, I. Omelchenko, A. Zakharova, and E. Schoell, "Delay controls chimera relay synchronization in multiplex networks," Phys. Rev. E **98**, 062224 (2018).
[24] I. Leyva, I. Sendina-Nadal, R. Sevilla-Escoboza, V. P. Vera-Avila, P. Chholak, and S. Boccaletti, "Relay synchronization in multiplex networks," Sci. Rep. **8**, 8629 (2018).
[25] S. Jalan, A. Kumar, and I. Leyva, "Explosive synchronization in frequency displaced multiplex networks," Chaos **29**, 041102 (2019).
[26] N. Li, X. Wu, J. Feng, Y. Xu, and J. Lü, "Fixed-time synchronization of coupled neural networks with discontinuous activation and mismatched parameters," IEEE Trans. Neural Netw. Learn. Syst. **32**(6), 2470–2482 (2021).

[27]N. Li, X. Wu, J. Feng, Y. Xu, and J. Lü, "Fixed-time synchronization of complex dynamical networks: A novel and economical mechanism," IEEE Trans. Cybern. (published online) (2020).
[28]X. Zhang, L. Tang, and L. Jinhu, "Synchronization analysis on two-layer networks of fractional-order systems: Intra-layer and inter-layer synchronization," IEEE Trans. Circuits Syst. I **67**, 2397–2408 (2020).
[29]Z. Tang, J. H. Park, and W.-X. Zheng, "Distributed impulsive synchronization of Lur'e dynamical networks via parameters variation methods," Int. J. Robust Nonlinear Control. **28**, 1001–1015 (2018).
[30]D. Yang, X. Li, and J. Qiu, "Output tracking control of delayed switched systems via state-dependent switching and dynamic output feedback," Nonlinear Anal. Hybrid Syst. **32**, 294–305 (2019).
[31]X. Li, X. Yang, and T. Huang, "Persistence of delayed cooperative models: Impulsive control method," Appl. Math. Comput. **342**, 130–146 (2019).
[32]G. Mei, X. Wu, D. Ning, and J. Lu, "Finite-time stabilization of complex dynamical networks via optimal control," Complexity **21**, 417–425 (2016).
[33]T. Nishikawa, A. E. Motter, Y. Lai, and F. C. Hoppensteadt, "Heterogeneity in oscillator networks: Are smaller worlds easier to synchronize?," Phys. Rev. Lett. **91**, 014101 (2003).
[34]C. Ma, Q. Yang, X. Wu, and J. Lu, "Cluster synchronization: From single-layer to multi-layer networks," Chaos **29**, 123120 (2019).
[35]M. Barahona and L. M. Pecora, "Synchronization in small-world systems," Phys. Rev. Lett. **89**, 054101 (2002).
[36]W. Lu, B. Liu, and T. Chen, "Cluster synchronization in networks of coupled nonidentical dynamical systems," Chaos **20**, 013120 (2010).
[37]Y. Li, X. Wu, J. Lu, and J. Lü, "Synchronizability of duplex networks," IEEE Trans. Circuits Syst. II **63**, 206–210 (2017).
[38]T. Njougouo, V. Camargo, P. Louodop, F. F. Ferreira, P. K. Talla, and H. A. Cerdeira, "Dynamics of multilayer networks with amplification," Chaos **30**, 123136 (2020).
[39]Y. Deng, Z. Jia, G. Deng, and Q. Zhang, "Eigenvalue spectrum and synchronizability of multiplex chain networks," Physica A **537**, 122631 (2019).
[40]L. Tang, J. Lu, and J. Lu, "A threshold effect of coupling delays on intra-layer synchronization in duplex networks," Sci. China Technol. Sci. **61**, 1907–1914 (2018).
[41]Y. Deng, Z. Jia, and F. Yang, "Synchronizability of multilayer star and star-ring networks," Discrete Dyn. Nat. Soc. **2020**(1), 1–20 (2020).
[42]M. Xu, J. Lu, and J. Zhou, "Synchronizability and eigenvalues of two-layer star networks," Neurocomput. **408**, 31–41 (2020).
[43]J. Aguirre, R. Sevilla-Escoboza, R. Gutiérrez, D. Papo, and J. Buldú, "Synchronization of interconnected networks: The role of connector nodes," Phys. Rev. Lett. **112**, 248701 (2014).
[44]L. Tang, X. Wu, J. Lu, J. Lu, and R. M. D'Souza, "Master stability functions for complete, intralayer, and interlayer synchronization in multiplex networks of coupled Rössler oscillators," Phys. Rev. E **99**, 012304 (2019).
[45]R. J. Mondragon, J. Iacovacci, and G. Bianconi, "Multilink communities of multiplex networks," PLoS One **13**, e0193821 (2018).
[46]S. Gomez, A. Diaz-Guilera, J. Gomez-Gardenes, C. J. Perez-Vicente, Y. Moreno, and A. Arenas, "Diffusion dynamics on multiplex networks," Phys. Rev. Lett. **110**, 028701 (2013).
[47]A. Tejedor, A. Longjas, E. Foufoula-Georgiou, T. T. Georgiou, and Y. Moreno, "Diffusion dynamics and optimal coupling in multiplex networks with directed layers," Phys. Rev. X **8**(3), 031071 (2018).
[48]S. Zhang, X. Wu, J. Lu, H. Feng, and J. Lu, "Recovering structures of complex dynamical networks based on generalized outer synchronization," IEEE Trans. Circuits Syst. I **61**, 3216–3224 (2014).
[49]M. Xu, J. Zhou, J. Lu, and X. Wu, "Synchronizability of two-layer networks," Eur. Phys. J. B **88**(9), 240 (2015).
[50]M. Xu, J. Lu, and J. Zhou, "Synchronizability and eigenvalues of two-layer star networks," Acta Phys. Sin. **65**, 383–395 (2016).
[51]P. Bonacich, "Factoring and weighting approaches to status scores and clique identification," J. Math. Sociol. **2**, 113–120 (1972).
[52]J. Iranzo, J. M. Buldu, and J. Aguirre, "Competition among networks highlights the power of the weak," Nat. Commun. **7**, 13273 (2016).
[53]P. Bonacich, "Power and centrality: A family of measures," J. Math. Sociol. **92**(5), 1170–1182 (1987).
[54]G. Sabidussi, "The centrality index of a graph," Psychometrika **31**, 581–603 (1966).
[55]X. Wu, W. Wei, L. Tang, J. Lu, and J. Lü, "Coreness and h-index for weighted networks," IEEE Trans. Circuits Syst. I **66**, 3113–3122 (2019).
[56]I. Leyva, R. Sevilla-Escoboza, I. Sendiña Nadal, R. Gutiérrez, J. M. Buldú, and S. Boccaletti, "Inter-layer synchronization in nonidentical multi-layer networks," Sci. Rep. **7**, 45475 (2017).
[57]L. C. Freeman, "A set of measures of centrality based on betweenness," Sociometry **40**, 35–41 (1977).
[58]A. D. Kachhvah, X. Dai, S. Boccaletti, and S. Jalan, "Interlayer Hebbian plasticity induces first-order transition in multiplex networks," New J. Phys. **22**(12), 122001 (2015).
[59]S. K. Dwivedi, M. S. Baptista, and S. Jalan, "Optimization of synchronizability in multiplex networks by rewiring one layer," Phys. Rev. E **95**, 040301 (2017).